Design of serially connected ammonia-water hybrid absorption-compression heat pumps for district heating with the utilisation of a geothermal heat source

Jensen, Jonas Kjær; Ommen, Torben Schmidt; Markussen, Wiebke Brix; Elmegaard, Brian

Published in:
Proceedings of ECOS 2016: 29th International Conference on Efficiency, Cost, Optimization, Simulation and Environmental Impact of Energy Systems

Publication date:
2016

Document Version
Peer reviewed version

Design of serially connected ammonia-water hybrid absorption-compression heat pumps for district heating with the utilisation of a geothermal heat source

Jonas K. Jensen[a], Torben Ommen[a], Wiebke B. Markussen[a] and Brian Elmegaard[a]

[a] Department of Mechanical Engineering – Technical University of Denmark, Kgs. Lyngby, Denmark, jkjje@mek.dtu.dk

Abstract:

District heating (DH) can reduce the primary energy consumption in urban areas with significant heat demands. The design of a serially connected ammonia-water hybrid absorption-compression heat pump system was investigated for operation in the Greater Copenhagen DH network in Denmark, in order to supply 7.2 MW heat at 85 °C utilizing a geothermal heat source at 73 °C. Both the heat source and heat sink experience a large temperature change over the heat transfer process, of which a significant part may be achieved by direct heat exchange. First a generic study with a simple representation of the heat pump was used to investigate optimal system configurations. It was shown that using two heat pumps in series with direct heat exchange in parallel with the first heat pump could increase the performance compared to a base case using direct heat exchange and a single heat pump, under the assumption that the exergetic efficiencies of the heat pumps are similar. Next, ammonia-water hybrid absorption-compression heat pumps were selected as heat pump technology, since these may increase the performance due the non-isothermal phase change. Detailed thermodynamic models predict that an exergetic efficiency of the system of 0.5 to 0.65 is possible. The technical feasibility as well as the economic viability of this installation was investigated for a range of preferred solutions. The analysis recommends a heat pump configuration with an exergetic efficiency of 0.63 which was within 2 % of the theoretical economic optimum.

Keywords:

Heat pump, district heating, hybrid absorption-compression, technical constraints.

1. Introduction

The municipality of Copenhagen, together with the Greater Copenhagen Area in Denmark, has the target to supply CO2 neutral district heating (DH) in 2025 [1]. The proposed method for achieving this target is mainly based on the conversion from fossil fuels to biomass in the large central combined heat and power (CHP) plants as well as incineration of waste in smaller CHP units. Waste incineration contributes as base load technology today and is expected to continue in the years to come, although with a slight decrease in available resources [2,3]. Focussing mainly on biomass as the sole fuel for intermittent and peak demand presents a significant risk in terms of security of supply [4]. Other supply technologies, such as heat pumps (HPs) utilising geothermal energy, or heat sources close to ambient, are also considered. It is expected that heat production capacity from HP technologies of approximately 300 MW is economically feasible, if appropriate heat sources can be located in the proximity of the DH network [5,6] .

Geothermal heat sources are used for a wide range of applications including both direct and indirect utilisation in district heating (DH) networks [7,8]. For utilisation in Danish DH systems, the temperature requirements for direct utilisation limits the possibilities and economic applicability [9]. However, by use of a geothermal heat source at a lower temperature than for direct utilisation, the temperature lift of the required heat pump is limited and may result in a favourable overall cost of heat. It may thus be a relevant alternative to biomass, but the technology is limited by drawbacks, such as a rather inflexible load profile due to the limitations of utilising the well, as well as the requirement for large investments to set up such systems.

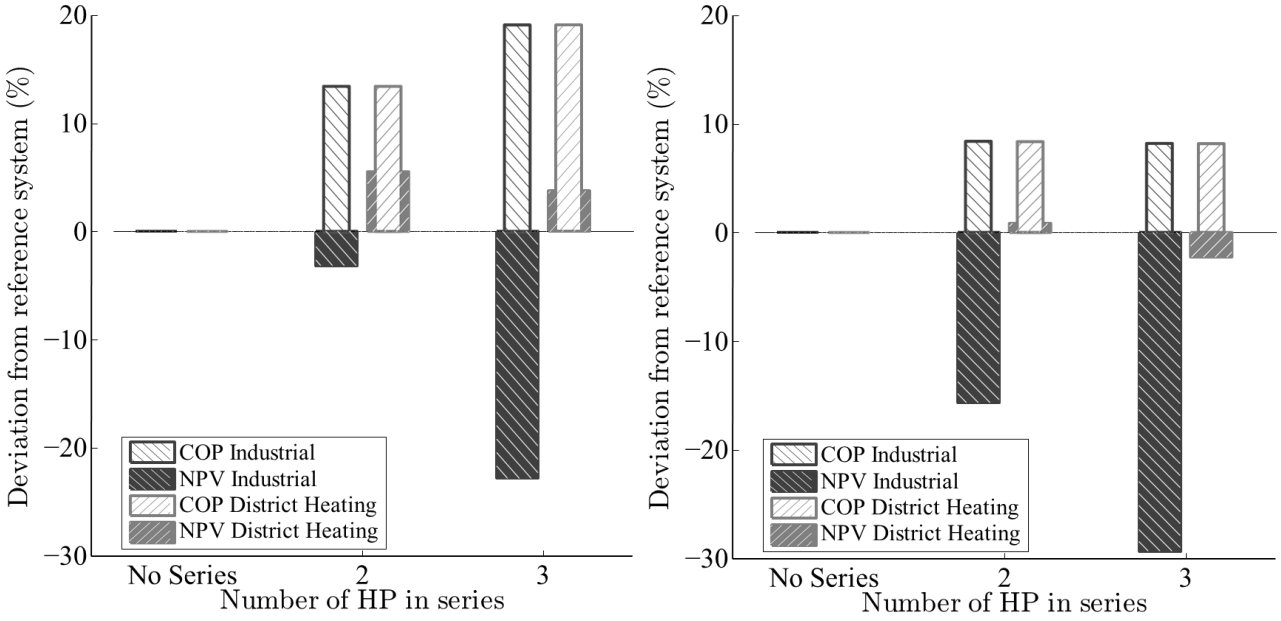

Fig. 1 Example of different economic performances of the number of HPs in series for two relevant cases in Danish energy system. The benefit of serial connection depends mainly on the economic case and the temperature difference of HP sink and source streams. (a) Serially connected HPs with overall sink temperature difference at 20 K and source temperature difference at 20 K. (b) Serially connected HPs with overall sink temperature difference at 40 K and source temperature difference at 10 K [14].

For applications in DH, the temperature variation of either source or sink stream is typically of a magnitude, where serial connection of HPs, may provide an increase in the coefficient of performance (COP) [10]. On the other hand, the economy of scale may suggest that the investment of a single unit is less than for two smaller units, when considering similar heat load. The most profitable solution may further vary with HP parameters such as sink temperature, temperature lift and temperature variation of sink and source streams.

Detailed thermo-economic models of various single stage vapour compression HPs (VCHP) were developed and investigated in Ommen et al [11]. The results are compared to similar results for the hybrid absorption-compression HP (HACHP) in [12]. The results show, that the best available technology in terms of net present value (NPV), typically depends on the performance and investment of the HP systems at the specific layout of the sink/source process streams. Besides the thermodynamic performance of the cycle and working fluid, it is important to consider the application limits of the individual components.

Possible benefits of integrating several HPs in series are presented in [13]. The analysis is performed for VCHPs using economic scenarios relevant for industrial integration/application. For such a case, the increased performance does not economically compensate for the increase in investment at the expected technical lifetime of the plant.

In the case of utility production in Denmark, a different taxation scheme is required for heat production compared to process heat for industry. The increased heat production cost for utilities, changes the economic optimum for a HP installation towards systems with higher COP to allow higher investment cost. In this way, the benefit of HPs operated in series becomes significant. To obtain low heat production prices, the utility companies are required to select utility plants with low consumer cost, where fuel (e.g. electricity) cost, market price of co-produced utilities (if any), O&M, taxes as well as investments are included in the calculation. An example of this difference between the two economic scenarios is presented in Fig. 1 for VCHPs [14].

It is shown, that the benefit of serial connection depends mainly on the economic case and the temperature difference of HP sink and source streams. All other relevant economic parameters are

similar to those presented in [13]. For the case of DH, it is shown that serial connection of two HPs is preferable for both of the presented sink and source temperature differences. At low source temperature difference, the benefit of serial connection is reduced to an insignificant increase considering the uncertainties of the analysis. At sink and source temperature differences of 20 K, the economic benefit is exceeding 5 %.

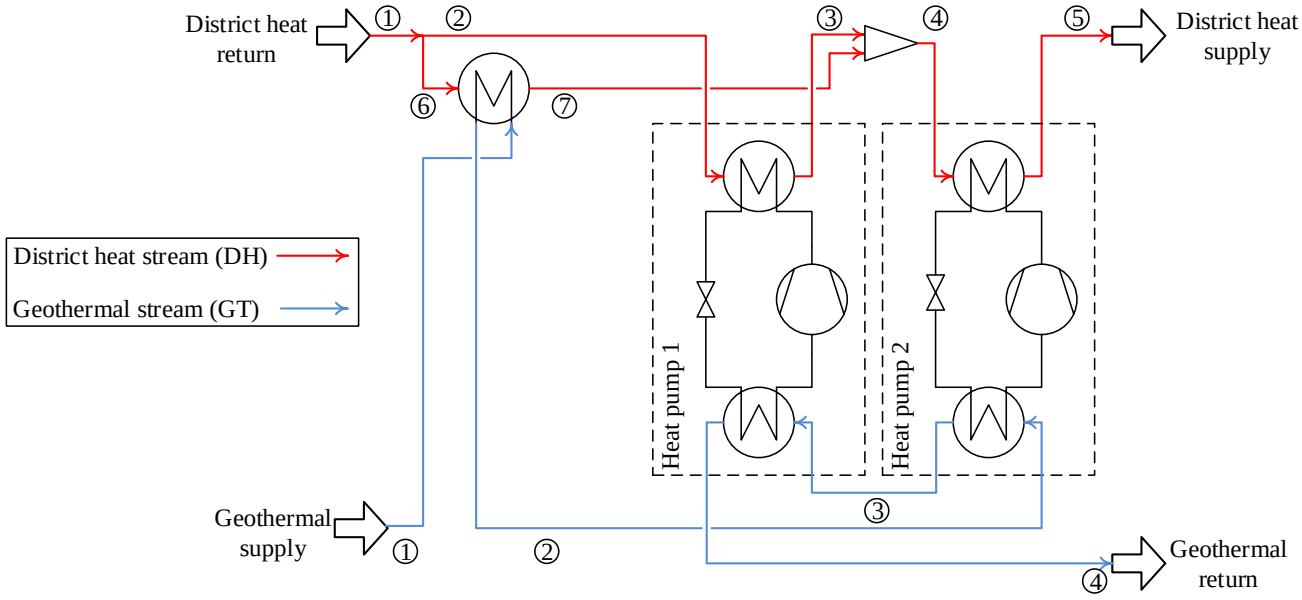

Fig. 2. Counter-current installation of two heat pumps

In case the temperature of the heat source is higher than the DH return, the system allows direct heat exchange (HEX) with the DH stream [15], which is preferable in terms of efficiency and cost. After utilising the possibility for direct HEX, the temperature differences exceed 20 K for both sink and source (approximately 30 K for both). For such high sink and source temperature differences, the analysis indicates, that the proposed setup (with VCHPs) should utilise two (or possibly three) HPs in series.

A simplified example of VCHP integration with a geothermal heat source is presented in Fig. 2. For integration of heat pumps in serial configuration, the counter-current configuration is preferable in terms of both energetic performance and technical constraints [13]. An example of a possible temperature – heat load diagram is presented in Fig. 3. The units are grouped by their integration with the heat sink. The flow of sink stream of HP1 and the direct HEX are mixed before being heated to the final specifications by HP2.

The analysis of the present study focusses on the possible increase in performance from the use of HP units operated in series alongside the utilisation of direct heat exchange with the heat source. Specifically, the performance improvements of both generic HP units and specific HACHPs are analysed and evaluated. The HACHP presents an interesting case, as the cycle configuration can be optimised for low entropy generation from heat exchange, compared to the isothermal vapour compression HPs. At the same time, the benefit from serial connection is closely related to the minimisation of entropy generation from the heat exchange, which implies that the possible benefit from operation in series may be lower for this type of HP. The performance of the serially connected HACHPs is further investigated in terms of the plant economy.

The analysis follows a three step increase in the level of detail of the performance evaluation. As an initial investigation, basic assumptions regarding the exergetic efficiency of the individual unit are applied to understand the influence of design parameters on the system exergy efficiency. Then a detailed thermodynamic model of the HACHP is used to predict the performance of the total installation. Finally, we analyse technical and economic considerations for best possible integration of two HACHPs in a range of exergy-optimal configurations.

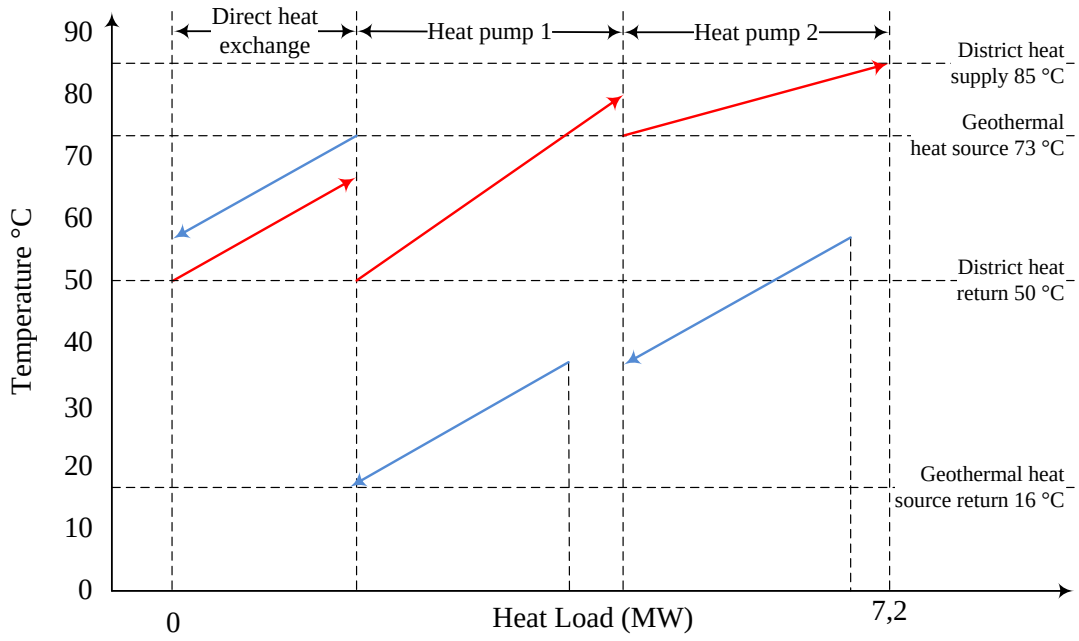

Fig. 3. Principal temperature – heat load diagram of counter-current configuration

2. Method

2.1. Case description

The design criteria for the geothermal heat pump are stated in Table 1. Here both the key economic parameters such as assumed lifetime, yearly operation hours etc. are stated along with the dimensioning temperature levels and heat loads.

The total system is designed to supply at total heat load of $\dot{Q}_{\mathrm{DH}} = 7.2$ MW to the district heating network. As direct heat exchange is imposed, the HPs will not deliver all 7.2 MW but only the remaining load, as seen in Eq. (1).

$$\dot{Q}_{\mathrm{HP,tot}} = \dot{Q}_{\mathrm{DH}} - \dot{Q}_{\mathrm{HEX}}, \quad (1)$$

The two heat pumps share the remaining load such that: $\dot{Q}_{\mathrm{HP,tot}} = \dot{Q}_{\mathrm{HP},1} + \dot{Q}_{\mathrm{HP},2}$. A HP heat load ratio, f_Q, was applied to determine the load share between the two heat pumps. The HP heat load ratio was defined as seen in Eq. (2).

$$f_Q = \frac{\dot{Q}_{\mathrm{HP},1}}{\dot{Q}_{\mathrm{HP,tot}}}, \quad (2)$$

Hence, if $f_Q = 0$ all HP heat load will be supplied by heat pump 2 while all HP heat load will be supplied by heat pump 1 if $f_Q = 1$.

As seen in Fig. 2 the district heating return stream is split before being heated by the HEX and HP 1, respectively. The mass flow ratio f_m was defined as the ratio between the mass flow supply to HP 1, $\dot{m}_{\mathrm{DH},2}$, and the total district heating mass flow rate, $\dot{m}_{\mathrm{DH},1}$, see Eq. (3).

$$f_m = \frac{\dot{m}_{\mathrm{DH},2}}{\dot{m}_{\mathrm{DH},1}}, \quad (3)$$

Hence, if $f_m = 0$ HP1 is bypassed and all mass flow is supplied to the HEX. Conversely, if $f_m = 1$, the HEX is bypassed and all mass flow is sent to HP 1.

The values of f_Q and f_m were to be determined in the design procedure. f_Q and f_m were determined to minimize the overall cost of the system, the Present Value (PV), under the constraints of commercially available components.

Table 1. Design criteria for the geothermal district heating plant

Basis for economic evaluation		Design temperature and heat loads	
Lifetime	20 years	$T_{\mathrm{DH,supply}} = T_{\mathrm{DH},5}$	85 °C
Yearly operating hours	3500 hours	$T_{\mathrm{DH,return}} = T_{\mathrm{DH},1}$	50 °C
Interest rate	4.5 %	$T_{\mathrm{GT,supply}} = T_{\mathrm{GT},1}$	73 °C
Inflation rate	1.9 %	$T_{\mathrm{GT,return}} = T_{\mathrm{GT},4}$	16 °C
Electricity cost	0.179 €/kWh	$\dot{Q}_{\mathrm{DH}}$	7.2 MW

2.2. Simple energy and exergy model of the geothermal installation

To determine the thermodynamic advantages of utilizing two heat pumps in series together with the direct heat exchange, a simple energy and exergy model of the installation was constructed. Using this model the thermodynamically optimal values of, f_Q and f_m were determined. If both optimal values are found to be between zero and unity it can be concluded that the configuration shown in Fig. 2 is advantageous.

Further, using this model it was investigated how the optimal values of f_Q and f_m were affected by the exergy efficiency of the individual heat pumps and the pinch point temperature difference of the HEX.

To construct the model it was assumed that the specific heat capacity, c_p, was constant and equal for both the district heating and geothermal stream, the value of c_p was evaluated for pure water at the average temperature in the system, $\bar{T} = \frac{1}{2}\left(T_{\mathrm{DH,supply}} + T_{\mathrm{GT,return}}\right)$. Pressure losses were neglected and the pressure of both the district heating stream and geothermal stream was assumed to be 5 bar.

For the exergy analysis the dead state temperature was assumed to be $T_0 = 16$ ℃, hence all streams depicted in Fig. 3 occur above the dead state temperature. As this was the case: all heated streams were viewed as product streams while all cooled streams were considered as fuel streams.

The thermal exergy difference of a heated stream was calculated as seen in Eq. (4) while Eq. (5) was applied to cooled streams.

$$\Delta\dot{E}_{\mathrm{Heated}} = \dot{m} \cdot c_p \cdot (T_{\mathrm{out}} - T_{\mathrm{in}}) - T_0 \cdot \dot{m} \cdot c_p \cdot \ln\frac{T_{\mathrm{out}}}{T_{\mathrm{in}}}, \quad (4)$$

$$\Delta\dot{E}_{\mathrm{Cooled}} = \dot{m} \cdot c_p \cdot (T_{\mathrm{in}} - T_{\mathrm{out}}) - T_0 \cdot \dot{m} \cdot c_p \cdot \ln\frac{T_{\mathrm{in}}}{T_{\mathrm{out}}}, \quad (5)$$

The exergy efficiency of components or systems was calculated as the of ratio of relevant exergetic product to the relevant exergetic fuel, as seen Eq. (6)

$$\varepsilon = \frac{\dot{E}_{\mathrm{product}}}{\dot{E}_{\mathrm{fuel}}}, \quad (6)$$

The direct heat exchange HEX was modelled as a counter flow heat exchanger, as seen in Fig. 2. The heat load of the HEX was determined by the pinch point temperature difference, $\Delta T_{\mathrm{pp,HEX}}$, defined as the minimum temperature difference in the HEX. As the HEX operates without phase change the $\Delta T_{\mathrm{pp,HEX}}$ can be determined as seen in Eq. (7).

$$\Delta T_{\mathrm{pp,HEX}} = \mathbf{min}\left(T_{\mathrm{GT},2} - T_{\mathrm{DH},6};\ T_{\mathrm{GT},1} - T_{\mathrm{DH},7}\right), \quad (7)$$

The heat load was subsequently determined from Eq. (8).

$$\dot{Q}_{\mathrm{HEX}} = \dot{m}_{\mathrm{DH},6} \cdot c_p \cdot \left(T_{\mathrm{DH},7} - T_{\mathrm{DH},6}\right) = \dot{m}_{\mathrm{GT},1} \cdot c_p \cdot \left(T_{\mathrm{GT},1} - T_{\mathrm{GT},2}\right), \quad (8)$$

The exergy efficiency of the HEX was found using Eqs. (4) - (6). The exergy product of the HEX is the heat supplied to the district heating stream and thus the exergy product can be found using Eq. (4). The exergy fuel is the heat supplied from the geothermal stream and is thus calculated using Eq. (5). The resulting exergy efficiency of the HEX can be seen in Eq. (9).

$$\varepsilon_{\mathrm{HEX}} = \frac{\dot{m}_{\mathrm{DH},6}}{\dot{m}_{\mathrm{GT},1}} \cdot \frac{\left(T_{\mathrm{DH},7} - T_{\mathrm{DH},6}\right) - T_0 \cdot \ln\left(\frac{T_{\mathrm{DH},7}}{T_{DH,6}}\right)}{\left(T_{\mathrm{GT},1} - T_{\mathrm{GT},2}\right) - T_0 \cdot \ln\left(\frac{T_{\mathrm{GT},1}}{T_{\mathrm{GT},2}}\right)}, \quad (9)$$

Both HPs in the system were treated equally. The COP of the heat pumps was determined from a given HP exergy efficiency, $\varepsilon_{\mathrm{HP}}$, and the operating conditions (DH/GT temperatures). For the analysis of the heat pumps, DH stream was termed the heat sink while the GT stream was termed the heat source.

The exergy product of the HP was assumed to be the heat supplied to the DH stream while the exergy fuel was the sum of the heat supplied from the GT stream and the supplied work, $\dot{W}_{\mathrm{HP}}$. Hence, the exergy efficiency of the HP was determined as seen in Eq. (10).

$$\varepsilon_{\mathrm{HP}} = \frac{\dot{m}_{\mathrm{DH}} \cdot c_p \cdot \left(T_{\mathrm{DH,out}} - T_{\mathrm{DH,in}}\right) - T_0 \cdot \dot{m}_{\mathrm{DH}} \cdot c_p \cdot \ln\frac{T_{\mathrm{DH,out}}}{T_{\mathrm{DH,in}}}}{\dot{m}_{\mathrm{GT}} \cdot c_p \cdot \left(T_{\mathrm{GT,in}} - T_{\mathrm{GT,out}}\right) - T_0 \cdot \dot{m}_{\mathrm{GT}} \cdot c_p \cdot \ln\frac{T_{\mathrm{GT,out}}}{T_{\mathrm{GT,in}}} + \dot{W}_{\mathrm{HP}}}, \quad (10)$$

By applying the definitions of the sink and source heat loads, $\dot{Q}_{\mathrm{sink}}$ and $\dot{Q}_{\mathrm{source}}$, Eqs. (11) & (12), as well as the definition of the logarithmic mean temperatures, $\bar{T}_{\mathrm{sink}}$ and $\bar{T}_{\mathrm{source}}$, Eq. (13), the HP exergy efficiency was reduced to the expression presented in Eq. (14).

$$\dot{Q}_{\mathrm{sink}} = \dot{m}_{\mathrm{DH}} \cdot c_p \cdot \left(T_{\mathrm{DH,out}} - T_{\mathrm{DH,in}}\right), \quad (11)$$

$$\dot{Q}_{\mathrm{source}} = \dot{m}_{\mathrm{GT}} \cdot c_p \cdot \left(T_{\mathrm{GT,in}} - T_{\mathrm{GT,out}}\right), \quad (12)$$

$$\bar{T}_{\mathrm{sink}} = \frac{T_{\mathrm{DH,out}} - T_{\mathrm{DH,in}}}{\ln\frac{T_{\mathrm{DH,out}}}{T_{\mathrm{DH,in}}}}, \quad \bar{T}_{\mathrm{source}} = \frac{T_{\mathrm{GT,in}} - T_{\mathrm{GT,out}}}{\ln\frac{T_{\mathrm{GT,in}}}{T_{\mathrm{GT,out}}}}, \quad (13)$$

$$\varepsilon_{\mathrm{HP}} = \frac{1 - \frac{T_0}{\bar{T}_{\mathrm{sink}}}}{1 - \frac{\dot{Q}_{\mathrm{source}}}{\dot{Q}_{\mathrm{sink}}} \cdot \frac{T_0}{\bar{T}_{\mathrm{source}}}}, \quad (14)$$

The COP of the HPs was defined as the ratio between the useful heat output $\dot{Q}_{\mathrm{sink}}$ and work input $\dot{W}_{\mathrm{HP}}$ by Eq. (15). Neglecting heat losses and assuming a steady state energy balance over the HP, further allowed the work input to be described as the difference between the sink and source heat load.

$$\mathrm{COP} = \frac{\dot{Q}_{\mathrm{sink}}}{\dot{W}_{\mathrm{HP}}} = \frac{\dot{Q}_{\mathrm{sink}}}{\dot{Q}_{\mathrm{sink}} - \dot{Q}_{\mathrm{source}}}, \quad (15)$$

Substituting Eq. (15) into Eq. (14) allows the COP to be determined from the exergy efficiency:

$$\mathrm{COP} = \left(1 - \frac{\bar{T}_{\mathrm{source}}}{T_0} \cdot \left(\frac{1}{\varepsilon_{\mathrm{HP}}} \cdot \left(\frac{T_0}{\bar{T}_{\mathrm{sink}}} - 1\right) + 1\right)\right)^{-1}, \quad (16)$$

The temperature after the mixing point situated between the two HPs, $T_{\mathrm{DH},4}$, was determined from a steady state energy balance. As the specific heat was assumed constant and the mass flow ratio, f_m, was defined, $T_{\mathrm{DH},4}$ was found as seen in Eq. (17)

$$T_{\mathrm{DH},4} = f_m \cdot T_{\mathrm{DH},3} + (1 - f_m) \cdot T_{\mathrm{DH},7}, \quad (17)$$

For the purpose of evaluating the exergetic performance of the mixing point the process was evaluated as a co-current heat exchanger with no temperature difference at the outlet. The sign of the difference between $T_{DH,3}$ and $T_{DH,7}$ depends on the value of f_Q and f_m and thus which stream is the exergetic fuel and which is exergetic product changes accordingly. The exergy efficiency of the mixing was calculated by either Eq. (18) or Eq. (19) according to the temperature levels of the incoming streams.

$$\textbf{if}: T_{DH,3} > T_{DH,7}: \varepsilon_{MX} = \frac{1-f_m}{f_m} \cdot \frac{(T_{DH,4}-T_{DH,7}) - T_0 \cdot \ln\frac{T_{DH,4}}{T_{DH,7}}}{(T_{DH,3}-T_{DH,4}) - T_0 \cdot \ln\frac{T_{DH,3}}{T_{DH,4}}}, \quad (18)$$

$$\textbf{if}: T_{DH,3} < T_{DH,7}: \varepsilon_{MX} = \frac{f_m}{1-f_m} \cdot \frac{(T_{DH,4}-T_{DH,3}) - T_0 \cdot \ln\frac{T_{DH,4}}{T_{DH,3}}}{(T_{DH,7}-T_{DH,4}) - T_0 \cdot \ln\frac{T_{DH,7}}{T_{DH,4}}}, \quad (19)$$

The exergy efficiency of the total installation was calculated as seen in Eq. (20). Here the entire heat load supplied to the DH stream was accounted as the exergy product, while the entire heat load supplied from the GT stream plus the power supplied to the two HPs was accounted as the exergy fuel.

$$\varepsilon_{tot} = \frac{\dot{m}_{DH,1} \cdot c_p \cdot (T_{DH,5}-T_{DH,1}) - T_0 \cdot \dot{m}_{DH,1} \cdot c_p \cdot \ln\frac{T_{DH,5}}{T_{DH,1}}}{\dot{m}_{GT,1} \cdot c_p \cdot (T_{GT,1}-T_{GT,4}) - T_0 \cdot \dot{m}_{GT,1} \cdot c_p \cdot \ln\frac{T_{GT,1}}{T_{GT,4}} + \dot{W}_{HP,1} + \dot{W}_{HP,2}}, \quad (20)$$

2.3. Hybrid absorption-compression heat pump

The main advantages of the HACHP is the non-isothermal phase-change induced by the use of a zeotropic working fluid as well as the reduction of vapour pressure compared to the vapour pressure of the pure volatile component. The non-isothermal phase-change is of significant importance in processes with large temperature difference over the heat sink and source. The reduction of vapour pressure is mainly an advantage for high temperature applications, but allows utilisation of equipment with lower technical constraints in terms of maximum high pressure. As seen in Fig. 3, the operating conditions for the two heat pumps are characterised by both large sink/source temperature differences and high operational temperatures, which makes the HACHP a relevant technology to investigate for the given case.

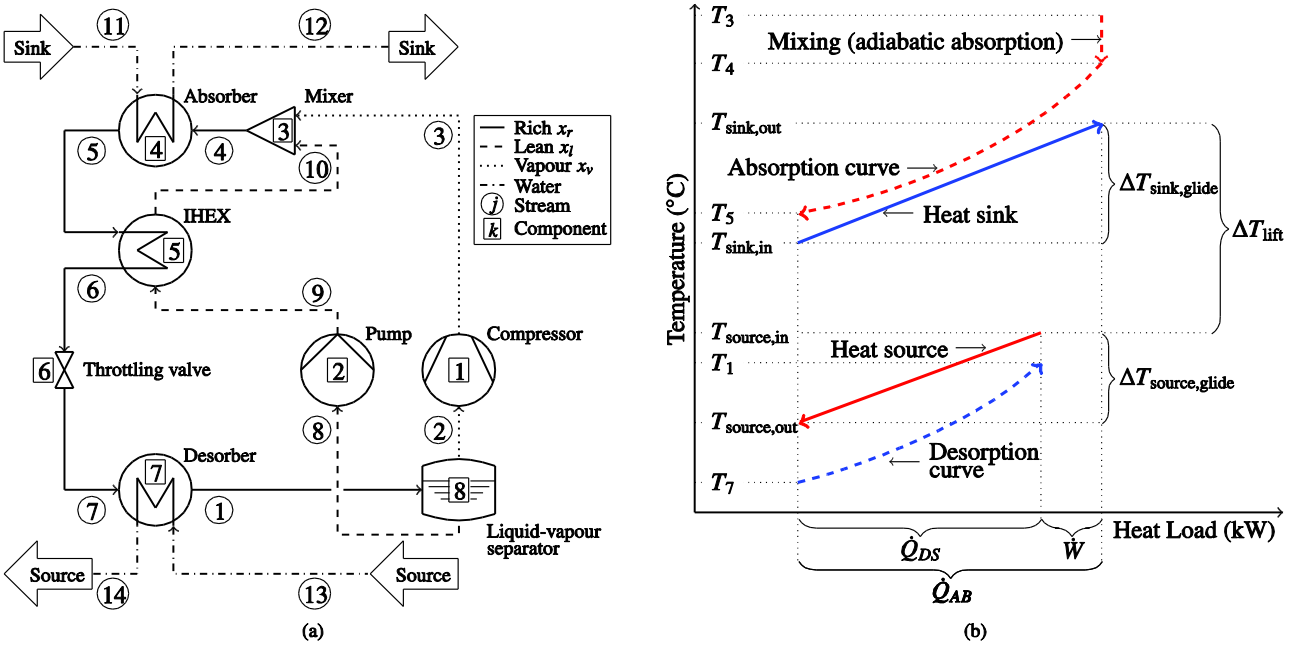

Fig. 4. (a) Principle sketch and (b) Temperature heat load diagram of HACHP

The general layout of the investigated HACHP may be seen in Fig. 4 (a). In the desorber heat is supplied from the heat source in order to desorb the ammonia from the mixture. The phase change in the desorber is incomplete and thus the stream exiting the desorber is a liquid/vapour mixture. By separating the phases in a liquid-vapour separator (LVS), it can be ensured that only the vapour phase enters the compressor, while the liquid phase is supplied to the pump. The liquid is preheated in the internal HEX, whereafter it is mixed with the vapour stream exiting the compressor. This causes an adiabatic absorption of the vapour phase into the liquid until thermodynamic equilibrium is reached. In the absorber a diabatic absorption of the ammonia vapour into the liquid is undertaken while releasing heat to the sink. The exiting stream is a saturated liquid mixture, which is used as the heat source in the internal HEX. The sub-cooled liquid mixture is throttled to the low pressure resulting in a two-phase stream that enters the desorber.

The process described above is sketched in the temperature – heat load diagram shown in Fig. 4 (b). Here the temperature lift, ΔT_{lift}, is defined as the difference between the sink outlet temperature (heat supply temperature) and the source inlet temperature. The temperature difference, ΔT , is defined as the temperature difference between the inlet and outlet of the sink and source, respectively.

The design of the HACHP is governed by two extra degrees of freedom compared to a conventional VCHP. These can be expressed by the choice of the rich ammonia mass fraction, x_r, and the choice of the liquid circulation ratio, f. The liquid circulation ratio was defined as the ratio between the mass flow rates of the lean and rich solution, see Fig. 4.

As shown in both [11] and [16] the choice of x_r and f affect both the system performance (COP) and the system investment. The optimum values of x_r and f depend on the HP operating conditions such as sink/source temperature differences as well as the temperature lift [11][15]. Further, x_r and f influence the technical constraints such as high pressure, p_H, and compressor discharge temperature, T_H. Thus, it is import to determine the correct combination of x_r and f in order to design an economically viable as well technically feasible heat pump solution.

Table 2. Inputs to the thermodynamic model of the HACHP as well as the technical constraints imposed to ensure the applicability of commercial components.

Thermodynamic model inputs			Technical constraints		
η_{is}	compressor	0,80 -	Low pressure NH_3 comp.	$p_{H,\max}$	28 bar
η_{is}	pump	0,80 -	High pressure NH_3 comp.	$p_{H,\max}$	50 bar
η_{elec}	electric motor efficiency	0,90 -	Compressor discharge temp.	$T_{H,\max}$	180 °C
ΔT_{pp}	absorber and desorber	5,0 K			
ϵ	Internal HEX	0,9 -			

The thermodynamic, heat transfer and economic models of the HACHP were implemented in Engineering Equation Solver (EES) [17] and follows the procedure presented in Jensen et al [11]. The inputs to the thermodynamic model may be seen in Table 2.

3. Results

The analysis was divided into three subsections, based on the level of detail of the performance evaluation for the individual heat pumps. The results are presented in terms of key operation criteria for the individual HP units heat load and flow configuration according to Eqs. (2) and (3).

- As an initial investigation, basic assumptions regarding the exergetic efficiency of the individual units were applied to understand the influence of design parameters on the system exergy efficiency. The results predict thermodynamic performance improvements for utilising certain configurations, compared to a simple system with only one HP and direct heat exchange.

- The use of a detailed thermodynamic model of the HACHP to predict the performance of the total installation. The results represent detailed information of both HPs and the direct HEX in a specific configuration. The performance improvement, as well as the method to obtain such improvement, was confirmed and refined.
- The use of technical and economic considerations for best possible integration of two HACHPs in a range of exergy-optimal configurations. This was done to analyse the influence of total capital investments, exergetic performance and technical constraints to achieve the minimum PV of a feasible plant.

3.1. Influence of design parameters on the system exergy efficiency

3.1.1. Heat pumps with equal efficiency $\varepsilon_{HP,1} = \varepsilon_{HP,2}$

For the case of equal exergetic efficiency in both HPs, an examination was performed to establish the optimal heat duty of each individual unit (HP1, HP2, Direct HEX) according to the principle diagram seen in Fig. 2. If operated without the direct HEX (f_Q=0), two heat pumps in series with fixed and equal exergetic efficiency will perform with a similar merit as one HP with the same efficiency. In such a case, the full flow of the DH passes through both HPs in succession. With increasing mass flow through the direct HEX, the heat load for the two heat pumps is decreased, but for many flow configurations this additionally leads to increased irreversibilites related to the mixing of the stream from HP1 and the direct HEX.

The performed analysis for the main configuration possibilities is presented in Fig. 5 (a) for HPs with exergetic efficiencies of 0.3 and a direct HEX with an allowable pinch temperature difference of 5 K. It is shown, that an optimum exist in a region with close to even heat distribution between the two HPs and close to even mass flow of DH steam (f_m ~ 0.6 in the direct HEX and HP1. At the optimum, the increase in exergy efficiency of the total installation is 0.05 compared to operating a HP at 0.3 exergetic efficiency alone (f_m = 1). On the other hand, a reduction of the performance by similar magnitude was possible due to mixing of a heated stream from HP1 with a colder stream from the direct HEX, seen for high values of f_Q and low values of f_m in Fig 5 (a). In case the full mass flow of DH stream is lead through the direct HEX (no flow through HP1) an increased performance of 0.03 was found. This result was similar to the performance at f_m=0.5. The optimal solution was identified to be a configuration with a balanced HEX, i.e. similar temperature differences at the inlet and outlet of the HEX, and lowest possible temperature difference between the two streams before mixing, resulting in low losses from mixing the heated streams of HEX and HP1

The benefit of optimal flow and heat load ratio was further dependent on the performance of the direct HEX and the performance of the HPs. In Fig 5 (b) various curves are presented for the optimal configurations for a range of exergetic efficiencies of the HPs and various possible minimum pinch differences in the direct HEX. It is seen that the overall system efficiency, ε_{tot}, is greatly influenced by the heat pump exergetic efficiency. However, the system performance can be improved by utilising two HPs and a direct HEX. As seen the improvements of the system when utilising a perfect HEX ($\Delta T_{pp,HEX}$= 0 K) was found to be higher than 0.05 and lower than 0.09 when varying the heat pump exergetic efficiency between 0.3 and 0.7. For a system with a high pinch point temperature difference ($\Delta T_{pp,HEX}$= 20 K) the performance improvements was found to be below 0.005 regardless of the performance of the HP units.

The optimal combinations of f_Q and f_m were determined for the considered range of HP exergetic efficiencies. The resulting load share and mass flow ratios are presented in Fig. 5 (c) and 5 (d). The optimum was found for all cases for a balanced heat exchanger. The thermal load of the direct HEX determines the optimal mixing temperature and the load of HP1 satisfies the required heating of the remaining mass flow, to minimise the losses from mixing.

With smaller pinch point temperature differences, more heat was transferred using the direct HEX, which allowed for higher loads on HP1. The highest load on HP1 was determined to be

approximately f_Q =0.5, but in reality the optimal heat load for this unit is lower due to the practical

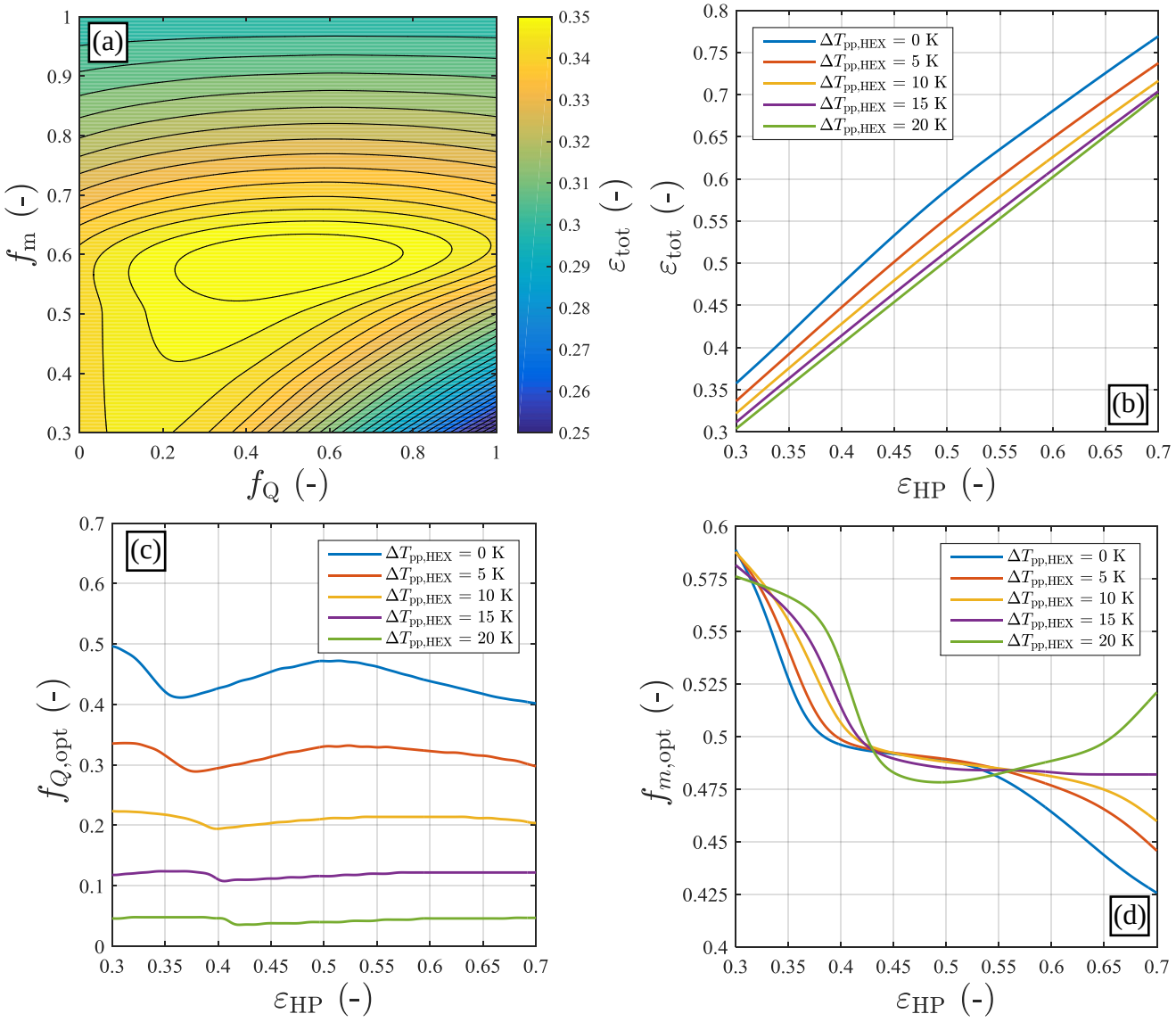

limitations in heat exchange. For the cases with poor pinch point characteristics in the direct HEX, the load of HP1 was found to be as low as 0.05.

Fig. 5 Performance of the proposed counter current configuration with two HPs with equal efficiency and a direct HEX. (a) Results presented for pinch temperature difference of 5 K.

3.1.2. Heat pumps with unequal efficiency $\varepsilon_{HP,1} \neq \varepsilon_{HP,2}$

The specific performance of a HP unit in terms of exergy efficiency can be considered a function of several independent factors, for example both the temperature levels and temperature difference of sink and source streams can be considered important [11]. Other factors include cycle configuration and the type and composition of the working fluid. For the configuration investigated here, variation of the factors f_m and f_Q will imply significantly changed operating conditions for each unit, and thus the exergetic efficiency is not fixed or equal for the two units.

Thus, in a real case, the preferred configuration differs from the above, as the system benefits from utilising the HP with the highest exergetic efficiency. However, by utilising the high exergy efficiency of a balanced direct HEX for a fraction of the heat load, a limited reduction in exergetic efficiency for one HP was found to be beneficial depending on the performance of the direct HEX. For the case of a direct HEX with a pinch point temperature difference of 5 K, the optimal configuration is presented in Fig. 6 (a). The figure reveals two large areas where only the HP with the highest exergetic efficiency should be utilised. The span where two HPs should be utilised is

wider at high exergy efficiencies than at lower efficiencies. The span was found to be slightly slanting, which showed preference for higher loads for HP2 than for HP1. The slanting is a result of the evaluated temperature levels, which for HP2 allows direct heat exchange between source and sink. In the case where HP2 operates with an efficiency of 0.5, the system benefits from utilising a second HP if the unit can operate with an efficiency between 0.45 and 0.5. Oppositely, in the case where HP1 operates with an efficiency of 0.5, the use of both heat pumps was beneficial for HP1 exergetic efficiency below 0.6, as HP2 includes the possibility for direct heat exchange. In case the HP1 efficiency is higher than this level, only HP1 should be utilised

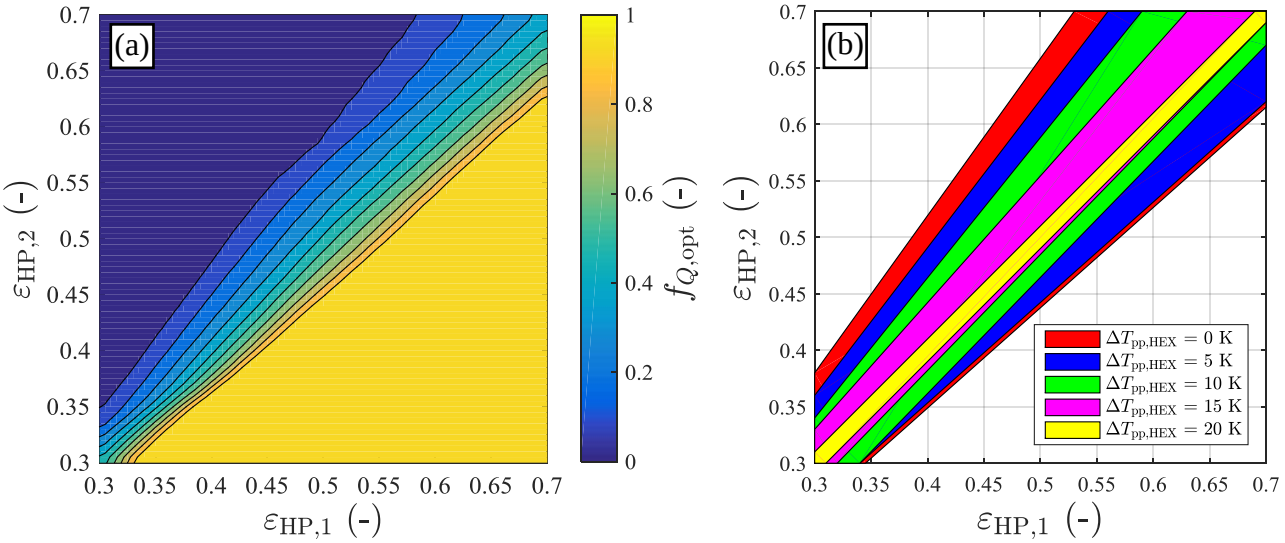

Fig. 6. Performance of the configuration with two HPs with unequal efficiency and a direct HEX ($\Delta T_{pp,HEX} = 5\ K$). (a) Optimal value of f_Q as a function of the HP exergetic efficienciency. In case of significant differences in the performance of the HPs, the optimal solutions include only one HP. (b) HPs efficiency combinations where two HPs are preferable ($0 < f_{Q,\mathrm{opt}} < 1$) for $\Delta T_{pp,HEX}$ from 0 K to 20 K

For configurations utilising the direct HEX, the pinch point temperature difference has a high influence on the feasible area for utilisation of both HPs. For configurations with poor heat exchanger characteristics, the optimum heat load share was shifted completely to the HP which allowed the highest exergy efficiency. The span where two HPs should be utilised is shown in Fig. 6 (b) for variation in pinch point temperature difference.

3.2. Hybrid Absorption Compression Heat Pump (HACHP)

By utilising a model for the specific HP technology, as well as the assumptions of component performance shown in Table 2, the assumed variations in individual HACHP unit exergetic performance reduced to an indication of the specific performance (according to the uncertainty of the thermodynamic model). For each of the considered HACHPs, the exergetic performance was optimised regarding the ammonia mass fraction of the individual units, x_r, and the liquid circulation ratio, f.

By calculating the total exergetic efficiency according to the specific operating criteria, a detailed inspection of the thermodynamic optimum was possible. The results of the performed analysis are presented in Fig. 7 for a pinch temperature difference in the direct HEX at 5 K.

For a pinch temperature difference in the direct HEX of 5 K, the total exergetic performance of the optimum was found to be approximately 0.64. The optimum is located at f_m = 0.48 and f_Q = 0.4 at which: $\varepsilon_{\mathrm{HP},1} = 0.547$ and $\varepsilon_{\mathrm{HP},2} = 0.615$. The choice of f_m corresponds to the specific mass flow required to obtain a balanced direct HEX for the specific temperatures of DH and geothermal source. The contours show, that such mass flow allows higher efficiencies for a wide range of heat load ratios. The optimal heat load ratio corresponds well to the previously established preference for heat load ratios below 0.5 (higher for HP2 than on HP1) from Section 3.1.2.

If, for other reasons, only one HP is preferred, the best performance is obtained at $f_Q = 0$, which restrict utilisation to only HP2. The optimal exergy efficiency for such operation was found to be 0.6, and can be obtained with either a balanced heat exchanger, $f_m = 0.48$, or an unbalanced heat exchanger, $f_m = 0$. In case of only one HP without a direct heat exchanger – either $f_Q = 0$ and $f_m = 1$ or $f_Q = 1$ and $f_m = 1$ – the exergetic efficiency is 0.53.

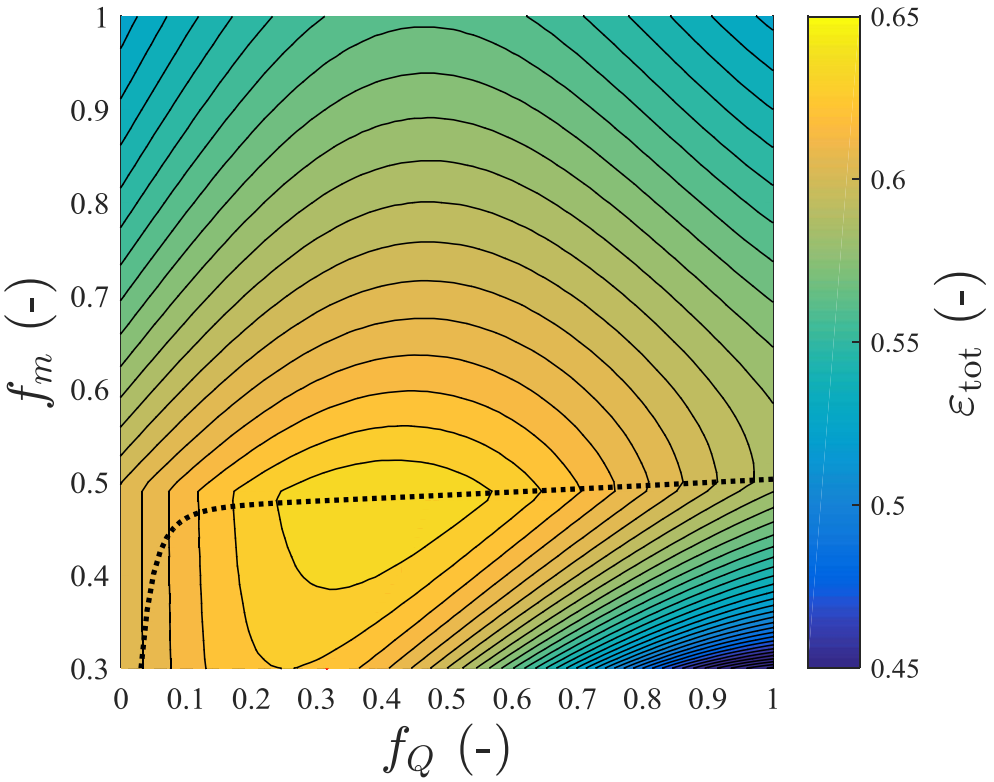

Fig. 7 Total exergetic efficiency of configurations with two HACHPs and a direct HEX. For each of the considered HACHPs, the exergetic performance was optimised regarding the ammonia mass fraction of the individual units and the liquid circulation ratio. The pinch temperature difference in the direct HEX was assumed at 5 K. The dotted line presents the optimal f_m according to the heat load ratio for achieving the highest exergy efficiency of the system.

3.3. Technical and economic considerations for best possible integration

For each of the individual configurations considered in Section 3.2, a set of operating conditions was derived, corresponding to each of the considered HACHP units. Component-specific technical constraints may limit the amount of feasible operating conditions if certain limits are exceeded. For this analysis two specific thermodynamic properties were considered as subject to constraints for feasible operation, according to the presented values of Table 2. High pressure components were identified to a limit of 50 (bar), whereas more conventional components typically operate below pressure constraints of 28 (bar). Components with high pressure requirements carry along additional investment according to a previous analysis [11,12]. Further, the considered compressors tend to be constrained by high discharge temperatures. For the analysis, the limitation was confined to below 180 °C, but other suppliers may require further reduction. For the HACHP technology, this technical limit is a significant obstacle in order to achieve high sink temperatures [12]. Based on the derived results of Section 3.2, the relation of optimal mass flow ratio was determined for a range of heat load ratios between 0.2 and 0.6. The range was chosen as this allows exergetic efficiencies of approximately 0.63 or above. The detailed operation of the two HPs, the direct heat exchanger and the total system is presented in Fig. 8. The heat loads of the individual units are presented in Fig 8

(a). For all of the optimised systems, the direct heat exchanger was responsible for transferring 1900 kW of heat. The remaining heat load (approx. 5300 kW) was split according to the heat load ratio.

The exergy efficiencies of the individual units, as well as the total, are presented in Fig. 8 (b). It is shown, that the exergy efficiency of the mixer is highest at approximately $f_Q = 0.35$ – meaning equal temperatures from both HP1 and the direct HEX. Above this ratio, the exergy destruction increases significantly as the heated DH stream from HP1 is mixed with a colder stream from the HEX. However, the exergy efficiency of both HPs increases with higher heat load ratio, which counterbalances the destruction in the mixer. As noted in Section 3.2, the total exergy efficiency is optimal at $f_Q = 0.4$. The variation of the exergetic efficiency of the total system was low, especially for f_Q between 0.3 and 0.45.

The technical parameters were identified for each HACHP based on the results of the investigated systems of Fig. 8. The constrained thermodynamic properties are presented in Fig. 9. The high pressure of the two cycles was well below the upper limit for both cases (50 bar), but at a heat load ratio of approximately 0.4 HP2 changes from low pressure to high pressure components in the high pressure stage. The range of heat load ratios is approximately 0.42 to 0.48.

The economic performance of the considered span of heat load ratios is presented in Fig. 10. In Fig. 10 (a) the capital investments for each of the units are presented, except for the mixer.

The investment for the direct HEX is quite limited compared to the total, less than 7 % for all cases, even though the required area is high due to the balanced temperature profile. For HP2 a shift in investment was encountered, when the components are changed for the high-pressure stage according to Fig 9 (a). It is further shown how the investments for the HPs correspond to the heat load ratio. The total investment cost for the system varies approximately 500.000 €, which is up to 18 % increase compared to the lowest possible.

In terms of present value (PV) of the total investment, the variation of the total system is approximately 650.000 €, with the location of the optimum (minimum) at $f_Q = 0.4$, which was identical with the location of the exergetic optimum. The variation of the PV in the investigated range of f_Q is below 5 % compared to the lowest cost.

In Table 3, the characteristics of the chosen operation point are presented. Detailed information on the HPs may be found in Appendix A. The technical constraints in terms of high discharge temperature shifted the chosen operating point away from the economic and exergetic optimum, as lower discharge temperatures are found for heat load ratios higher than 0.42. The chosen operating point represents a HP with exergetic efficiency of 0.63 which was within 2 % of the theoretical economic optimum.

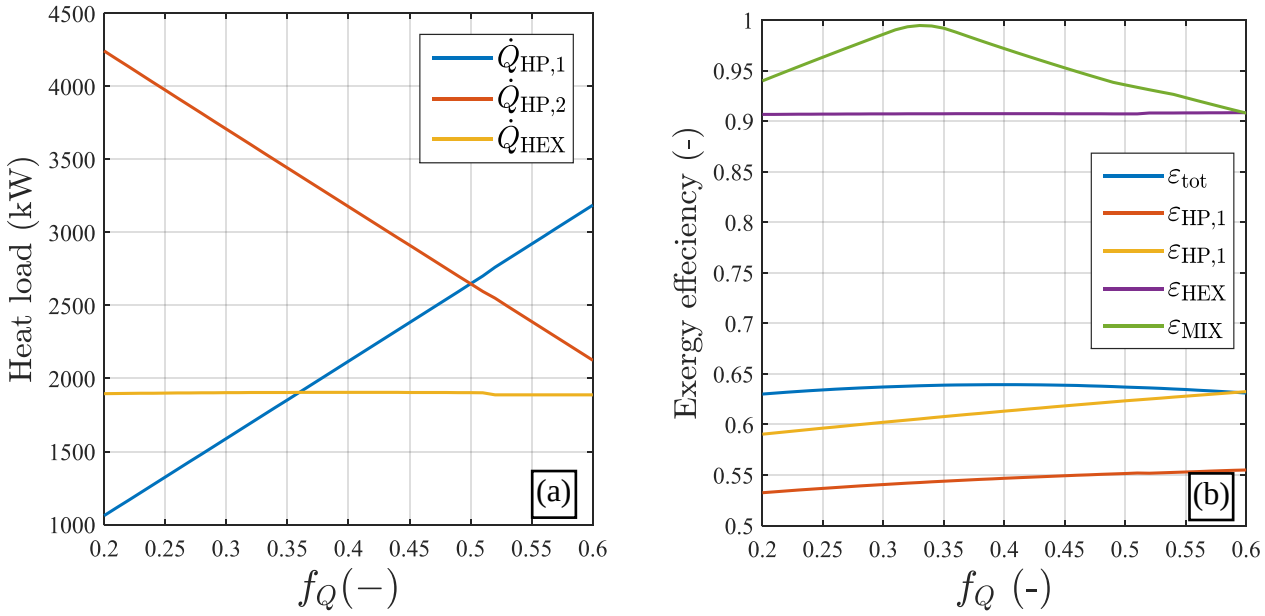

Fig. 8 Operation of the two HACHPs for a range of load ratio configurations with optimal mass flow ratio to achieve best exergetic efficiency. (a) Individual unit load (b) Individual and total exergy efficiency.

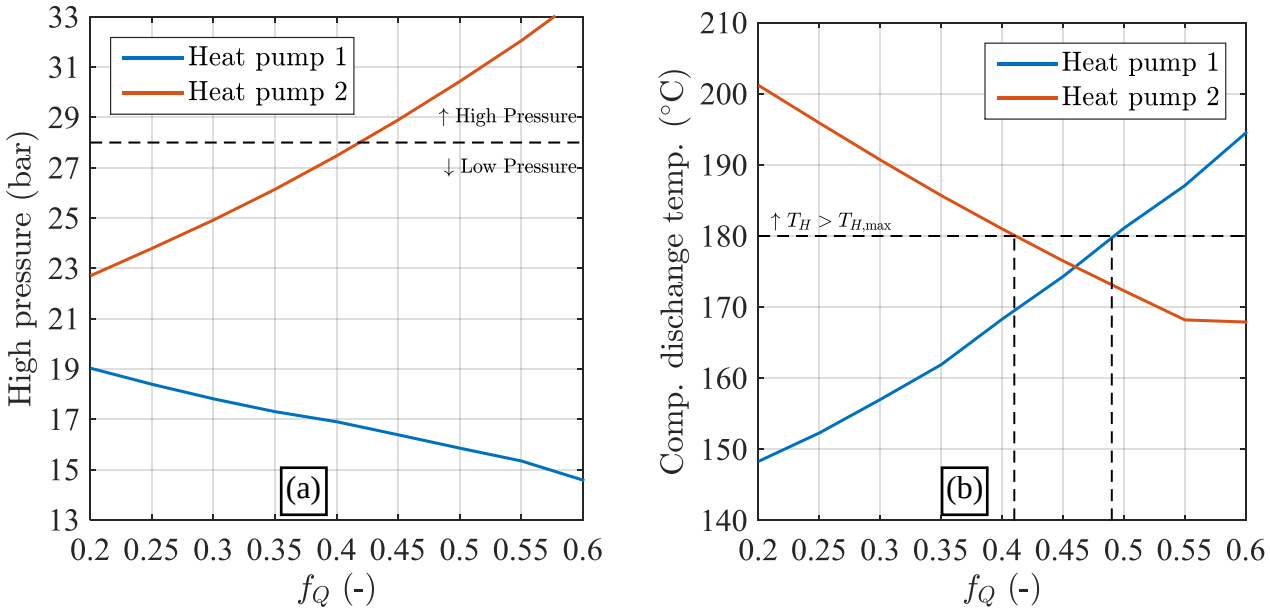

Fig. 9 Technical constraints of the two HACHPs for a range of load ratio configurations with optimal mass flow ratio to achieve best exergetic efficiency. (a) High pressure of HP1 and HP2 (b) Compressor discharge temperature of HP1 and HP2.

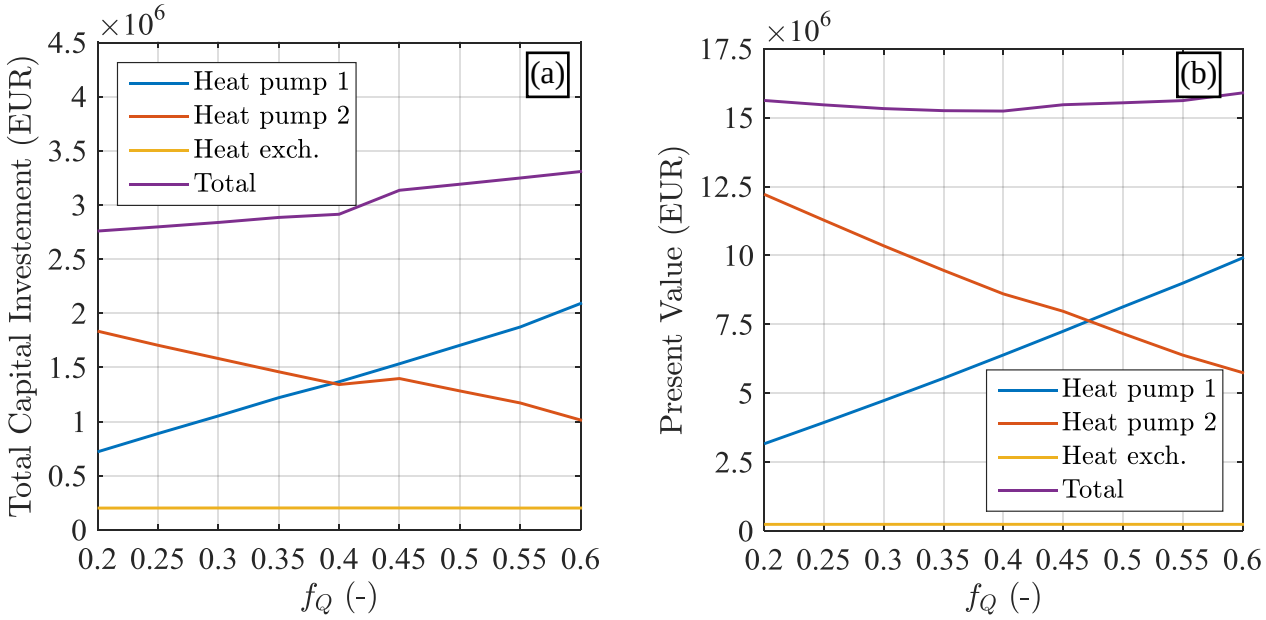

Fig. 10 Economic performance of the two HACHPs for a range of load ratio configurations with optimal mass flow ratio to achieve best exergetic efficiency.

Table 3 System characteristics at the chosen operation point. The optimum in terms of PV was challenged by the technical constraints, which required f_Q higher than 0.42.

Heat pump 1		Heat pump 2		Heat exchanger	
x_r	0.689 -	x_r	0.772 -	$\dot{Q}_{\mathrm{HEX}}$	1904 kW
f	0.637 -	f	0.493 -	$\varepsilon_{\mathrm{HP}}$	0.912 -
p_H	16.4 bar	p_H	28.9 bar	TCI	203,430 €
T_H	174 °C	T_H	176 °C		
$\dot{Q}_{\mathrm{sink}}$	2225 kW	$\dot{Q}_{\mathrm{sink}}$	3071 kW		
COP	4,36 -	COP	4,58 -		
$\varepsilon_{\mathrm{HP}}$	0.544 -	$\varepsilon_{\mathrm{HP}}$	0.613 -		
TCI	1,466,225 €	TCI	1,439,220 €		
Total system					
$\varepsilon_{\mathrm{tot}}$	0.634 -				
TCI	3,108,875 €				
PV	15,430,000 €				

4. Discussion

The analysis followed a three step increase in the level of detail of the performance evaluation for the investigated HPs. For all three investigations, the results showed a performance gain for utilising a balanced heat exchanger alongside two heat pumps in series. The initial analysis showed that a maximal improvement of 9 percentage points in terms of exergy efficiency was possible from optimal implementation of the direct HEX, but at the same time, that the highest heat share should be placed on the HP with the best figure of merit. When using detailed models to predict the performance of the HACHP, the real performance improvement from optimal integration was shown to be 0.04. In terms of economy, the minimal PV was found for the same flow configuration. Due to technical constraints, specifically the high discharge temperature of the compressors, a feasible configuration was proposed, although with slightly higher investment costs. The chosen operating point represents a HP with exergetic efficiency of 0.63 which was within 2 % of the

theoretical economic optimum. It should however be expected that the uncertainties of model input, such as e.g. design criteria, component and fuel costs, as well as mathematical representation of the individual components, may offset the theoretical economic optimum.

In the cases where VCHPs were used for the analysis, the system would likely be subject to lower exergetic efficiencies for each HP, due to isothermal phase change characteristics in the heat exchangers. The performance improvement from optimal implementation of the direct HEX would be similar. A feasible method to avoid excess entropy generation from VCHPs in processes with high temperature difference are to increase the number of serially connected HPs, but with the drawback of increased investment due to the economy of scale, which would demand a recalculation of the technical and economically optimal configuration.

4. Conclusion

The design of a serially connected ammonia-water hybrid absorption-compression heat pump was investigated for operation in the Greater Copenhagen DH network, in order to supply 7.2 MW heat utilizing a geothermal heat source at 73 °C. Both the heat source and heat sink will experience a large temperature change over the heat transfer process, of which a significant part can be achieved by direct heat exchange. The investigated heat pump configuration may increase the performance due to the non-isothermal phase change. The benefit was further assisted by the use of HPs in series. The analysis was divided into three subsections, based on the level of detail of the performance evaluation for the individual heat pumps. The results were presented in terms of key operation criteria for the heat load and flow configuration of the individual HP units. Detailed thermodynamic models predicted that an exergetic efficiency of 0.5 (-) to 0.65 (-) was possible. The technical feasibility as well as the economic viability of this installation was investigated for a range of preferred solutions. The chosen operating point represents a HP with exergetic efficiency of 0.63 (-) which was within 2 % of the theoretical economic optimum.

Acknowledgments

This research project is financially funded by EUDP (Energy Technology Development and Demonstration). Project title: “Experimental development of electric heat pumps in the Greater Copenhagen DH system - Phase 1", project number: 64014-0127

Nomenclature

Abbreviations

EES	engineering equation solver
HACHP	hybrid absorption-compression heat pump
VCHP	vapour compression heat pump
HP	heat pump
DH	district heating
CHP	combined heat and power
HEX	heat exchanger
NPV	net present value
PV	present value
TCI	total capital investment

Symbols

c_p	specific heat,	kJ/(kg K)
COP	coefficient of performance	-
$\dot{m}$	mass flow rate,	kg/s

p	pressure,	bar
T	temperature,	°C
ΔT	temperature difference,	K
$\dot{Q}$	heat rate,	kW
$\dot{W}$	work rate,	kW
x	ammonia mass fraction,	-
f	Circulation rate,	-
f_m	mass flow ratio,	-
f_Q	heat load ratio,	-

Greek symbols

ε	exergy efficiency	-
ϵ	heat exchanger effectiveness	-
η	efficiency	-

Subscripts and superscripts

H	high
HP	heat pump
r	rich
l	lean
v	vapour

References

[1] City Council of Copenhagen. CPH Climate Plan 2025 (In danish: KBH 2025 Klimaplan - En grøn, smart og CO2-neutral by.) 2013.http://kk.sites.itera.dk/apps/kk_pub2/pdf/983_jkP0ekKMyD.pdf

[2] Ommen T, Markussen WB, Elmegaard B. Lowering district heating temperatures – Impact to system performance in current and future Danish energy scenarios. Energy 2016;94:273–291. doi:10.1016/j.energy.2015.10.063.

[3] CTR, HOFOR and VEKS. Heat Plan Greater Copenhagen 3 (in Danish: Varmeplan Hovedstaden 3) 2014. http://www.varmeplanhovedstaden.dk/files/otherfiles/0000/0124/VPH3_Hovedrapport_-_oktober_2014.pdf

[4] Mathiesen BV, Lund H, Connolly D. Limiting biomass consumption for heating in 100% renewable energy systems. Energy 2012;48:160–8. doi:10.1016/j.energy.2012.07.063.

[5] Bach B, Werling J, Ommen T, Münster M, Morales MM, Elmegaard B. Integration of large-scale heat pumps in the district heating systems of Greater Copenhagen, Energy 2016;107:321–334.

[6] CTR, HOFOR and VEKS. Heat Plan Greater Copenhagen 3 (in Danish: Varmeplan Hovedstaden 3) 2014. http://www.varmeplanhovedstaden.dk/files/otherfiles/0000/0124/VPH3_Hovedrapport_-_oktober_2014.pdf

[7] Lund JW, Freeston DH. World-wide direct uses of geothermal energy 2000. Geothermics 2001;30:29–68. doi:10.1016/S0375-6505(00)00044-4.

[8] Hepbasli A. A review on energetic, exergetic and exergoeconomic aspects of geothermal

district heating systems (GDHSs). Energy Convers Manag 2010;51:2041–61. doi:10.1016/j.enconman.2010.02.038.

[9] Østergaard PA, Lund H. A renewable energy system in Frederikshavn using low-temperature geothermal energy for district heating. Appl Energy 2011;88:479–87. doi:10.1016/j.apenergy.2010.03.018.

[10] Prestmark V, Schultz J. Planning and design of a 15 MW geothermal heat pump installation in Denmark. heat pumps Build., 1984, p. 171–87.

[11] Ommen T, Jensen JK, Markussen WB, Reinholdt L, Elmegaard B. Technical and economic working domains of industrial heat pumps: Part 1 - single stage vapour compression heat pumps. Int J Refrig 2015.

[12] Jensen JK, Ommen T, Markussen WB, Reinholdt L, Elmegaard B. Technical and economic working domains of industrial heat pumps 2: Ammonia-Water hybrid absorption-compression heat pumps. Int J Refrig 2015:-. doi:http://dx.doi.org/10.1016/j.ijrefrig.2015.02.011.

[13] Ommen T, Kj J, Markussen WB, Elmegaard B. Enhanced technical and economic working domains of industrial heat pumps operated in series, International Congress of Refrigeration ICR, Yokohama, Japan, 2015.

[14] Grüner S, Elmegaard B, Ommen T, Rothuizen ED, Jensen JK, Christensen C, et al. Experimental development of electric heat pumps in the Greater Copenhagen DH system - Phase 1. Copenhagen: 2016.

[15] Berntsson T. Heat sources - Technology, economy and environment. Int J Refrig 2002;25:428–38. doi:10.1016/S0140-7007(01)00034-2.

[16] Jensen JK, Markussen WB, Reinholdt L, Elmegaard B. On the development of high temperature ammonia–water hybrid absorption–compression heat pumps. Int J Refrig 2015;58:79–89. doi:10.1016/j.ijrefrig.2015.06.006.

[17] Klein SA. Engineering Equation Solver Academic Professional V9.459-3D 2013.

Appendix A: detailed outputs for the best possible design

Table 4. State points for HP1 under the suggested design conditions

$\dot{m}_j$ (kg/s)	p (bar)	T (°C)	s (kj/kg-K)	h (kJ/kg)	x (-)	v (m^3/kg)
4,1405	3,589	27,59	1,973	414,78	0,689	1,44E-01
1,505	3,589	27,59	4,982	1344,1	0,997	3,93E-01
1,505	16,38	174,3	5,128	1662,5	0,997	1,28E-01
4,14	16,38	81,77	2,318	611,34	0,689	3,61E-02
4,14	16,38	58,53	0,752	74,13	0,689	1,41E-03
4,14	16,38	41,70	0,506	-5,42	0,689	1,37E-03
4,14	3,589	11,00	0,538	-5,42	0,689	4,08E-02
2,635	3,589	27,59	0,255	-116,0	0,513	1,22E-03
2,635	16,38	27,78	0,257	-114,0	0,513	1,22E-03
2,635	16,38	55,49	0,654	10,94	0,513	1,26E-03
22,04	10	50,00	0,703	210,2	-	-
22,04	10	74,13	1,004	311,1	-	-
23,905	10	33,41	0,483	140,8	-	-
23,905	10	16	0,239	68,05	-	-

Table 5. State points for HP1 under the suggested design conditions

$\dot{m}_j$ (kg/s)	p (bar)	T (°C)	s (kj/kg-K)	h (kJ/kg)	x (-)	v (m^3/kg)
4,554	7,946	48,94	2,663	687,08	0,772	9,42E-02
2,307	7,946	48,94	4,706	1372,36	0,996	1,85E-01
2,307	28,88	176,51	4,829	1645,3	0,996	7,08E-02
4,554	28,88	104,75	2,928	881,94	0,772	2,96E-02
4,554	28,88	76,11	1,061	207,45	0,772	1,56E-03
4,554	28,88	65,13	0,902	152,5	0,772	1,52E-03
4,554	7,946	28,41	0,944	152,5	0,772	2,59E-02
2,247	7,946	48,94	0,566	-16,52	0,542	1,27E-03
2,247	28,88	49,35	0,568	-13,19	0,542	1,27E-03
2,247	28,88	73,47	0,901	98,17	0,542	1,32E-03
51,765	10	70,84	0,965	297,32	-	-
51,765	10	85	1,134	356,66	-	-
26,977	10	55	0,767	231,08	-	-
26,977	10	33,41	0,483	140,83	-	-

Table 6. Heat transfer area, mean temperature difference and pressure loss for the plate heat exchangers of HP1 and HP2 under the suggested design conditions.

	$\dot{Q}$ (kW)	Area (m^2)	$\Delta\bar{T}$ (°C)	Δp hot side (bar)	Δp cold side (bar)
Heat Pump 1					
Absorber	2224,5	132,5	5,939	0,0005499	0,0495
Desorber	1740	166,3	6,543	0,00819	0,000581
IHEX	329,4	31,46	7,155	0,006767	0,002784
Heat Pump 2			0		
Absorber	3071,5	90,3	7,227	0,001514	0,4978
Desorber	2434,5	163,7	7,733	0,00659	0,0007233
IHEX	250,2	13,645	7,339	0,04018	0,009719